Structural Engineering and Mechanics, Vol. 15, No. 2 (2003) 249-267
DOI: http://dx.doi.org/10.12989/sem.2003.15.2.249

Analysis of circular plates on two - parameter elastic foundation

Ahmet Saygun† and Mecit Çelik‡

Faculty of Civil Engineering, Istanbul Technical University, Maslak 80626 Istanbul, Turkey

(Received October, 2001, Accepted October, 2002)

Abstract. In this study, circular plates subjected to general type of loads and supported on a two-parameter elastic foundation are analysed. The stiffness, elastic bedding and soil shear effect matrices of a fully compatible ring sector plate element, developed by Saygun (1974), are obtained numerically assuming variable thickness of the element. Ring sector soil finite element is also defined to determine the deflection of the soil surface outside the domain of the plate in order to establish the interaction between the plate and the soil. According to Vallabhan and Das (1991) the elastic bedding (C) and shear parameters (C_T) of the foundation are expressed depending on the elastic constants (E_s, ν_s) and the thickness of compressible soil layer (H_s) and they are calculated with a suitable iterative procedure. Using ring sector elements presented in this paper, permits the generalization of the loading and the boundary conditions of the soil outside the plate.

Key words: ring sector compatible plate finite element; the coefficient of subgrade reactions; shear parameter coefficient; mode shape parameter.

1. Introduction

As known, in order to perform a better model than the Winkler hypothesis Pasternak (1954), Vlasov and Leontev (1966) developed a two-parameter model elastic foundation and analysed beams and slabs on it. Vlasov, in his model, introduced a parameter γ to characterize the distribution of the vertical displacement in the elastic foundation. Jones and Xenophontes (1977) using variational principles, strengthened the Vlasov model by establishing a relationship between the parameter γ and the displacements of the beam or slab on the foundation. Vallabhan *et al*. (1988, 1991) developed an iterative technique to determine the γ parameter numerically for beams and rectangular plates on elastic foundations. Vallabhan and Daloğlu (1997) employed the finite element method. Four-noded rectangular finite elements with 12 degrees-of-freedom are developed to model the slab and the soil along with four degrees-of-freedom elements for the beams that stiffen the slab. Brown (1969), Burmister (1956) studied circular rafts on a elastic foundation under uniformly distributed load. Vallabhan and Das (1991) extended their model for the analysis of axial symmetric circular tank foundation. Finite element solution given by Çelik and Saygun (1999) used the similar

† Professor
‡ Associate Professor

iteration principle, given by Vallabhan, to determine the γ parameter and the deflections of the soil around the plate was also considered.

In this study, using the full compatible ring sector finite element developed by Saygun (1974), this method is extended to circular plates subjected to general loading.

2. Governing equation of circular plates on two parameter foundation

The governing equation of the deflection of the plate $w(r, \theta)$ on a two- parameter elastic foundations can be expressed as

$$D\Delta\Delta w - 2C_T\Delta w + Cw = q \tag{1}$$

where D is the flexural rigidity of the plate $[D = E_p h_p^3/12(1 - \nu_p^2)]$, q external load on the plate, C the elastic bedding coefficient and $2C_T$ the shear parameter coefficient. Laplacian operator Δ in the polar coordinates is.

$$\Delta = \frac{\partial^2}{\partial r^2} + \frac{1}{r}\frac{\partial}{\partial r} + \frac{1}{r^2}\frac{\partial^2}{\partial \theta^2} \tag{2}$$

The governing equation for the deflection of the soil surface outside the domain of the plate becomes,

$$-2C_T\Delta w + Cw = 0 \tag{3}$$

The mode shape function $\phi(z)$ defining the variation of the vertical displacement in the vertical direction inside the soil layer, has the boundary conditions:

$$\phi(z = 0) = 1, \qquad \phi(z = H) = 0 \tag{4}$$

where H is the thickness of the compressible soil layer supposed to be known.

By minimizing the total potential energy function by $\phi(z)$ in the domain of the soil $(0 \le z \le H)$, the function $\phi(z)$ can be expressed as

$$\phi(z) = \frac{\sinh[\gamma(1 - z/H)]}{\sinh\gamma} \tag{5}$$

where γ denotes the mode shape parameter. Furthermore, the elastic bedding coefficient C and the shear parameter coefficient $2C_T$ can be obtained as follows depending on the mode shape parameter γ:

$$C = \frac{E_s(1 - \nu_s)}{(1 + \nu_s)(1 - 2\nu_s)}\frac{\gamma}{H}\frac{[\sinh 2\gamma + 2\gamma]}{4\sinh^2\gamma} \tag{6}$$

$$2C_T = G_s\frac{H}{\gamma}\frac{[\sinh 2\gamma - 2\gamma]}{4\sinh^2\gamma} \tag{7}$$

where E_s, ν_s and G_s are the elastic constants of the soil. The mode shape parameter γ is determined in polar coordinates as follows:

$$\gamma^2 = H^2 \frac{(1-2\nu)}{2(1-\nu)} \frac{\int_{r=0}^{\infty} \int_{\theta=0}^{2\pi} \left\{ \left(\frac{\partial w(r,\theta)}{\partial r} \right)^2 + \left(\frac{\partial w(r,\theta)}{r \partial \theta} \right)^2 \right\} r dr d\theta}{\int_{r=0}^{\infty} \int_{\theta=0}^{2\pi} w^2(r,\theta) r dr d\theta} \tag{8}$$

As seen in Eqs. (6)-(8) the elastic bedding coefficient (C) and the shear parameter coefficient (C_T) depend on the material properties, the thickness of compressible layer of the soil and the coefficient γ. On the other hand, γ depends on the deflection shape of the system, subjected to the external load. It is obvious that the iterative method, suggested by Vallabhan and Das (1991), has to be used in the numerical solution. By assuming an initial value for γ the coefficients C and $2C_T$ can be computed and the system, combined with plate and soil finite elements, is analysed. Then a new γ can be computed by using Eq. (8) and the procedure is repeated until the difference between the two successive values of γ will be less than a prescribed value.

3. Fully compatible ring sector plate element

Consider a ring sector plate as shown in Fig. 1. As in the case of the rectangular plate element developed by Bogner *et al.* (1966), a deflection function that ensures both the deflection and slope compatibility at the boundaries of ring sector element must be expressed at least with 16 nodal degrees of freedom,

$$w = \sum_{i=1}^{16} w_i(r,\theta) d_i \tag{9}$$

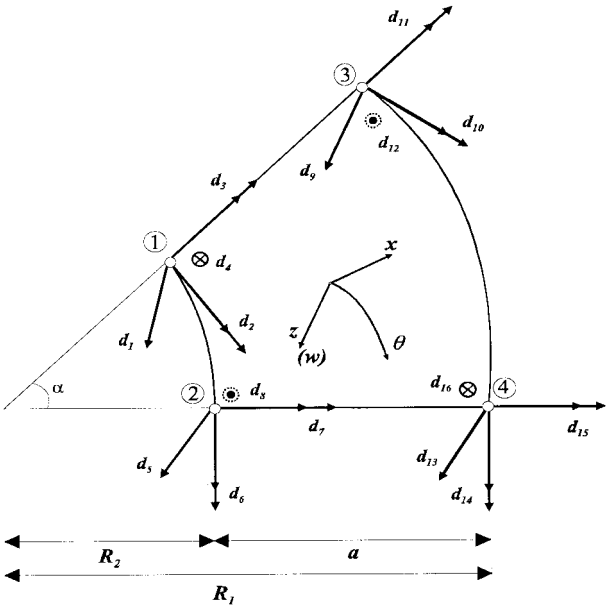

Fig. 1 Ring sector plate finite element

or in matrix form

$$w = [A_d][d] \tag{10}$$

where $[d]$ is a column matrix of nodal displacements and $[A_d]$ is a line matrix which contains 6 corresponding displacement functions on the element.

The numbering and sign convention of nodal displacements, which are the vertical displacement, two slopes in radial and circumferential directions and torsional curvatures $\partial^2 w/\partial r(r\partial\theta)$ at each node, are shown in Fig. 1.

The functions $w_i(r, \theta)$, that determine the displacement shape on the element due to unit nodal freedoms, are product of functions in radial and angular directions.

Choosing the origin of the variable x at the middle radius, the radial coordinate at any point of the element can be expressed as

$$r = x + (R_1 + R_2)/2 \tag{11}$$

and setting

$$a = R_1 - R_2 \tag{12}$$

the variation in radial direction can be expressed with a simple third order polynomial of x.

The four polynomial expressions corresponding to unit deflection or slope at the ends $r = R_1$ ($x = a/2$) and $r = R_2$ ($x = -a/2$) are given below:

Function	Boundary Condition	
$f_1(x) = \frac{1}{2} + \frac{3x}{2a} - \frac{2x^3}{a^3}$	$\begin{cases} f_1 = 1 \text{ and } df_1/dx = 0 \text{ for } x = a/2 \\ f_1 = 0 \text{ and } df_1/dx = 0 \text{ for } x = -a/2 \end{cases}$	(13a)
$f_2(x) = \frac{1}{2} - \frac{3x}{2a} + \frac{2x^3}{a^3}$	$\begin{cases} f_2 = 0 \text{ and } df_2/dx = 0 \text{ for } x = a/2 \\ f_2 = 1 \text{ and } df_2/dx = 0 \text{ for } x = -a/2 \end{cases}$	(13b)
$g_1(x) = \frac{a}{8} + \frac{x}{4} - \frac{x^2}{2a} - \frac{x^3}{a^2}$	$\begin{cases} g_1 = 0 \text{ and } dg_1/dx = -1 \text{ for } x = a/2 \\ g_1 = 0 \text{ and } dg_1/dx = 0 \text{ for } x = -a/2 \end{cases}$	(13c)
$g_2(x) = -\frac{a}{8} + \frac{x}{4} + \frac{x^2}{2a} - \frac{x^3}{a^2}$	$\begin{cases} g_2 = 0 \text{ and } dg_2/dx = 0 \text{ for } x = a/2 \\ g_2 = 1 \text{ and } dg_2/dx = -1 \text{ for } x = -a/2 \end{cases}$	(13d)

In angular direction the functions have to contain trigonometric functions such as $\sin\theta$ and $\cos\theta$ to satisfy rigid body motion. For this reason the shape functions depending on θ are chosen as follows instead of third order polynomial function:

$$w = a_1 + a_2\theta + a_3\cos\theta + a_4\sin\theta \tag{14}$$

The coefficients a_i can be found by using the corresponding boundary conditions at $\theta = \mp\alpha/2$. The functions and their corresponding boundary conditions are listed as follows:

Function Boundary Condition

$$\varphi_1(\theta) = \frac{1}{2} + \frac{\sin(\theta) - \theta\cos\frac{\alpha}{2}}{2\left(\sin\frac{\alpha}{2} - \frac{\alpha}{2}\cos\frac{\alpha}{2}\right)} \qquad \begin{cases} \varphi_1 = 1 & \text{and} \quad \partial\varphi_1/\partial\theta = 0 \quad \text{for} \quad \theta = \alpha/2 \\ \varphi_1 = 0 & \text{and} \quad \partial\varphi_1/\partial\theta = 0 \quad \text{for} \quad \theta = -\alpha/2 \end{cases} \tag{15a}$$

$$\varphi_2(\theta) = \frac{1}{2} - \frac{\sin(\theta) - \theta\cos\frac{\alpha}{2}}{2\left(\sin\frac{\alpha}{2} - \frac{\alpha}{2}\cos\frac{\alpha}{2}\right)} \qquad \begin{cases} \varphi_2 = 0 & \text{and} \quad \partial\varphi_2/\partial\theta = 0 \quad \text{for} \quad \theta = \alpha/2 \\ \varphi_2 = 1 & \text{and} \quad \partial\varphi_2/\partial\theta = 0 \quad \text{for} \quad \theta = -\alpha/2 \end{cases} \tag{15b}$$

$$\psi_1(\theta) = \frac{\cos(\theta) - \cos\frac{\alpha}{2}}{2\sin\frac{\alpha}{2}} - \frac{\theta\sin\frac{\alpha}{2} - \frac{\alpha}{2}\sin(\theta)}{2\left(\sin\frac{\alpha}{2} - \frac{\alpha}{2}\cos\frac{\alpha}{2}\right)} \qquad \begin{cases} \psi_1 = 0 & \text{and} \quad \partial\psi_1/\partial\theta = -1 \quad \text{for} \quad \theta = \alpha/2 \\ \psi_1 = 0 & \text{and} \quad \partial\psi_1/\partial\theta = 0 \quad \text{for} \quad \theta = -\alpha/2 \end{cases} \tag{15c}$$

$$\psi_2(\theta) = -\frac{\cos(\theta) - \cos\frac{\alpha}{2}}{2\sin\frac{\alpha}{2}} - \frac{\theta\sin\frac{\alpha}{2} - \frac{\alpha}{2}\sin(\theta)}{2\left(\sin\frac{\alpha}{2} - \frac{\alpha}{2}\cos\frac{\alpha}{2}\right)} \qquad \begin{cases} \psi_2 = 0 & \text{and} \quad \partial\psi_2/\partial\theta = 0 \quad \text{for} \quad \theta = \alpha/2 \\ \psi_2 = 0 & \text{and} \quad \partial\psi_2/\partial\theta = -1 \quad \text{for} \quad \theta = -\alpha/2 \end{cases} \tag{15d}$$

The matrix $[A_d]$ in Eq. (10) consists of combination of functions mentioned above.

$$\begin{aligned} [A_d] = [& \varphi_2(\theta)f_2(x) \quad \varphi_2(\theta)g_2(x) \quad -\psi_2(\theta)rf_2(x) \quad \psi_2(\theta)rg_2(x) \\ & \varphi_1(\theta)f_2(x) \quad \varphi_1(\theta)g_2(x) \quad -\psi_1(\theta)rf_2(x) \quad \psi_1(\theta)rg_2(x) \\ & \varphi_2(\theta)f_1(x) \quad \varphi_2(\theta)g_1(x) \quad -\psi_2(\theta)rf_1(x) \quad \psi_2(\theta)rg_1(x) \\ & \varphi_1(\theta)f_1(x) \quad \varphi_1(\theta)g_1(x) \quad -\psi_1(\theta)rf_1(x) \quad \psi_1(\theta)rg_1(x)] \end{aligned} \tag{16}$$

This deflection function satisfies rigid body motion conditions and the case of axial symmetry. Consequently the stiffness matrix derived from these functions successfully passes all the patch tests.

4. Stiffness matrix

Internal forces of the element can be obtained as follows depending on displacement shape in polar coordinate.

$$\begin{bmatrix} M_r \\ M_\theta \\ M_{r\theta} \end{bmatrix} = \underbrace{\frac{Eh^3}{12(1-\nu^2)} \begin{bmatrix} 1 & \nu & 0 \\ \nu & 1 & 0 \\ 0 & 0 & \frac{1-\nu}{2} \end{bmatrix}}_{[D]} \underbrace{\begin{Bmatrix} -\frac{\partial^2 w}{\partial r^2} \\ -\left(\frac{\partial^2 w}{r^2\partial\theta^2} + \frac{\partial w}{r\partial r}\right) \\ -2\frac{\partial w}{\partial r}\left(\frac{\partial w}{r\partial\theta}\right) \end{Bmatrix}}_{[\partial]} \tag{17}$$

As known the stiffness matrix of the plate element in bending [k], which relates nodal forces to nodal displacements as

$$[P] = [k][d] \tag{18}$$

can be determined as follows by using the virtual work principle:

$$[k] = \iint [A_d]^T [\partial]^T [D][\partial][A_d] dA \tag{19}$$

The coefficients of the matrix [k] in polar coordinates is given below.

$$\begin{aligned} k_{ij} = D \int_{R_2}^{R_1} \int_{-\frac{\alpha}{2}}^{\frac{\alpha}{2}} \Bigg\{ & \frac{\partial^2 w_i}{\partial r^2}\frac{\partial^2 w_j}{\partial r^2} + \left(\frac{\partial^2 w_i}{r^2 \partial \theta^2} + \frac{\partial w_i}{r \partial r}\right)\left(\frac{\partial^2 w_j}{r^2 \partial \theta^2} + \frac{\partial w_j}{r \partial r}\right) \\ & + \nu \left[\frac{\partial^2 w_i}{\partial r^2}\left(\frac{\partial^2 w_j}{r^2 \partial \theta^2} + \frac{\partial w_j}{r \partial r}\right) + \frac{\partial^2 w_j}{\partial r^2}\left(\frac{\partial^2 w_i}{r^2 \partial \theta^2} + \frac{\partial w_i}{r \partial r}\right) \right] \\ & + 2(1-\nu)\left(\frac{\partial^2 w_i}{r \partial \theta \partial r} - \frac{\partial w_i}{r^2 \partial \theta}\right)\left(\frac{\partial^2 w_j}{r \partial \theta \partial r} - \frac{\partial w_j}{r^2 \partial \theta}\right) \Bigg\} r dr d\theta \end{aligned} \tag{20}$$

Specially if the thickness of the element is assumed variable, numerical integration using Gaussian weighting coefficients is suitable to compute the stiffness matrix.

5. Stress-nodal displacement relation

When the system has been analysed for the nodal displacements, the curvatures at each nodes can be obtained as follows:

$$[\chi]_b = [B_b][d] \tag{21}$$

where each column of the matrix [B_b] denotes the curvatures at the nodes due to unit nodal displacement. The bending and twisting moments can be computed as follows

$$[M_d] = [D][B_b][d] \tag{22}$$

By using the following abbreviation.

$$e_1 = \frac{\sin\frac{\alpha}{2}}{2\left(\sin\frac{\alpha}{2} - \frac{\alpha}{2}\cos\frac{\alpha}{2}\right)}, \quad e_2 = \frac{1}{2}\operatorname{cotan}\frac{\alpha}{2} + \frac{\alpha}{2}e_1, \quad e_3 = -\frac{1}{2}\operatorname{cotan}\frac{\alpha}{2} + \frac{\alpha}{2}e_1 \tag{23}$$

The matrix [B_b] is given in Table 1 where χ_s, χ_θ and 2τ denote the bending curvatures in radial and angular direction and the torsion curvatures, respectively.

Table 1 Ring sector deformation matrix

		$[d]_1$				$[d]_2$				$[d]_3$				$[d]_4$			
Nod	$[\chi]$	d_1	d_2	d_3	d_4	d_5	d_6	d_7	d_8	d_9	d_{10}	d_{11}	d_{12}	d_{13}	d_{14}	d_{15}	d_{16}
	χ_s	$\frac{6}{a^2}$	$-\frac{4}{a}$	0	0	0	0	0	0	$-\frac{6}{a^2}$	$-\frac{2}{a}$	0	0	0	0	0	0
1	χ_θ	$\frac{e_1}{R_2^2}$	$\frac{1}{R_2}$	$\frac{e_2}{R_2}$	0	$-\frac{e_1}{R_2^2}$	0	$\frac{e_3}{R_2}$	0	0	0	0	0	0	0	0	0
	2τ	0	0	0	–2	0	0	0	0	0	0	0	0	0	0	0	0
	χ_s	0	0	0	0	$\frac{6}{a^2}$	$-\frac{4}{a}$	0	0	0	0	0	0	$-\frac{6}{a^2}$	$-\frac{2}{a}$	0	0
2	χ_θ	$-\frac{e_2}{R_2^2}$	0	$-\frac{e_3}{R_2}$	0	$\frac{e_1}{R_2^2}$	$\frac{1}{R_2}$	$-\frac{e_2}{R_2}$	0	0	0	0	0	0	0	0	0
	2τ	0	0	0	0	0	0	0	–2	0	0	0	0	0	0	0	0
	χ_s	$-\frac{6}{a^2}$	$\frac{2}{a}$	0	0	0	0	0	0	$\frac{6}{a^2}$	$\frac{4}{a}$	0	0	0	0	0	0
3	χ_θ	0	0	0	0	0	0	0	0	$\frac{e_1}{R_1^2}$	$\frac{1}{R_1}$	$\frac{e_2}{R_1}$	0	$-\frac{e_1}{R_1^2}$	0	$\frac{e_3}{R_1}$	0
	2τ	0	0	0	0	0	0	0	0	0	0	0	–2	0	0	0	0
	χ_s	0	0	0	0	$-\frac{6}{a^2}$	$\frac{2}{a}$	0	0	0	0	0	0	$\frac{6}{a^2}$	$\frac{4}{a}$	0	0
4	χ_θ	0	0	0	0	0	0	0	0	$-\frac{e_1}{R_1^2}$	0	$-\frac{e_3}{R_1}$	0	$\frac{e_1}{R_1^2}$	$\frac{1}{R_1}$	$-\frac{e_2}{R_1}$	0
	2τ	0	0	0	0	0	0	0	0	0	0	0	0	0	0	0	–2

6. Elastic bedding and shear parameter matrices

The inclusion of elastic bedding and shear effect of the soil to the equilibrium equation of the plate element can be made easily using the procedure adopted by Çelik and Saygun (1999). The final equation becomes

$$[P] = [k][d] + [C][d] + [C_T][d] \tag{24}$$

where $[C]$ and $[C_T]$ are the elastic bedding and shear effect matrices. Their terms can be expressed as follows:

$$C_{ij} = C\int_{R_2}^{R_1}\int_{-\frac{\alpha}{2}}^{\frac{\alpha}{2}} w_i w_j r dr d\theta \tag{25}$$

$$C_{Tij} = 2C_T\int_{R_2}^{R_1}\int_{-\frac{\alpha}{2}}^{\frac{\alpha}{2}}\left\{\frac{\partial w_i}{\partial r}\frac{\partial w_j}{\partial r} + \frac{\partial w_i}{r\partial\theta}\frac{\partial w_j}{r\partial\theta}\right\} r dr d\theta \tag{26}$$

They will be computed numerically just as the stiffness matrix.

7. Ring sector soil element

In the present study a finite element of ring sector shape is used also to determine the deflection surface of the soil. The governing differential equation outside the domain of the plate Eq. (3) denotes an analogy behaviour of shear plate which has a shear rigidity $Gh' = 2C_T$ and layed on elastic foundation having an elastic bedding coefficient C. The displacement shape can be defined with four d.o.f. shown in Fig. 2, in the following form

$$w_s = [A_d]_s[d]_s \tag{27}$$

The shape functions of the element consist of linear functions in radial direction and equivalent to linear function in angular direction. These functions are listed below.

Function	Boundary Conditions	
$l_1(x) = (0.5 + x/a)$	$l_1(x = a/2) = 1, \quad l_1(x = -a/2) = 0$	(28a)
$l_2(x) = (0.5 - x/a)$	$l_2(x = a/2) = 0, \quad l_2(x = -a/2) = 1$	(28b)
$\lambda_1(\theta) = \frac{1}{2} + \frac{\sin\theta}{2\sin\frac{\alpha}{2}}$	$\lambda_1(\theta = \alpha/2) = 1, \quad \lambda_1(\theta = -\alpha/2) = 0$	(28c)
$\lambda_2(\theta) = \frac{1}{2} - \frac{\sin\theta}{2\sin\frac{\alpha}{2}}$	$\lambda_2(\theta = \alpha/2) = 0, \quad \lambda_2(\theta = -\alpha/2) = 1$	(28d)

The matrix $[A_d]_s$ depending on above functions is given as follows.

$$[A_d]_s = [\lambda_2(\theta)l_2(x) \quad \lambda_1(\theta)l_2(x) \quad \lambda_2(\theta)l_1(x) \quad \lambda_1(\theta)l_1(x)] \tag{29}$$

Elastic bedding and shear parameter matrices in ring sector soil finite element can be computed as follows in polar coordinates.

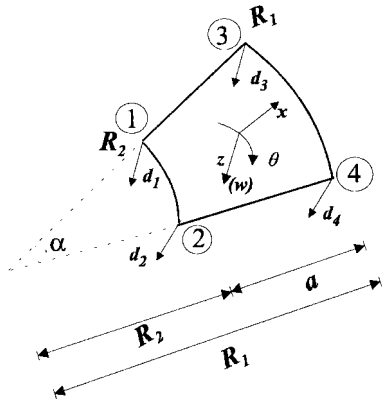

Fig. 2 Ring sector soil finite element

$$C_{i,j} = C\int_{R_2}^{R_1}\int_{-\frac{\alpha}{2}}^{\frac{\alpha}{2}} w_i w_j r dr d\theta \tag{30}$$

$$C_{Ti,j} = 2C_T\int_{R_2}^{R_1}\int_{-\frac{\alpha}{2}}^{\frac{\alpha}{2}}\left\{\frac{\partial w_i}{\partial r}\frac{\partial w_j}{\partial r} + \frac{\partial w_i}{r\partial\theta}\frac{\partial w_j}{r\partial\theta}\right\} r dr d\theta \tag{31}$$

These matrices is given below.

$$[C] = \begin{bmatrix} C_{11} & C_{12} & C_{13} & C_{14} \\ C_{21} & C_{22} & C_{23} & C_{24} \\ C_{31} & C_{32} & C_{33} & C_{34} \\ C_{41} & C_{42} & C_{43} & C_{44} \end{bmatrix}, \quad [C_T] = \begin{bmatrix} C_{T11} & C_{T12} & C_{T13} & C_{T14} \\ C_{T21} & C_{T22} & C_{T23} & C_{T24} \\ C_{T31} & C_{T32} & C_{T33} & C_{T34} \\ C_{T41} & C_{T42} & C_{T43} & C_{T44} \end{bmatrix} \tag{32}$$

The terms of elastic bedding and shear parameter matrices are found as follows.

$$C_{11} = C\left\{\frac{(R_1 - R_2)(R_1 + 3R_2)}{48}\left(\alpha + \frac{\alpha - \sin\alpha}{1 - \cos\alpha}\right)\right\} = C_{22} \tag{33a}$$

$$C_{12} = C\left\{\frac{(R_1 - R_2)(R_1 + R_2)}{48}\left(\alpha + \frac{\sin\alpha - \alpha}{1 - \cos\alpha}\right)\right\} \tag{33b}$$

$$C_{13} = C\left\{\frac{(R_1^2 - R_2^2)}{48}\left(\alpha + \frac{\alpha - \sin\alpha}{1 - \cos\alpha}\right)\right\} = C_{24} \tag{33c}$$

$$C_{14} = C\left\{\frac{(R_1^2 - R_2^2)}{48}\left(\alpha + \frac{\sin\alpha - \alpha}{1 - \cos\alpha}\right)\right\} = C_{23} \tag{33d}$$

$$C_{33} = C\left\{\frac{(R_1 - R_2)(3R_1 + R_2)}{48}\left(\alpha + \frac{\alpha - \sin\alpha}{1 - \cos\alpha}\right)\right\} = C_{44} \tag{33e}$$

$$C_{34} = C\left\{\frac{(R_1 - R_2)(3R_1 + R_2)}{48}\left(\alpha + \frac{\sin\alpha - \alpha}{1 - \cos\alpha}\right)\right\} \tag{33f}$$

The terms of shear parameter matrix. (34a….34g)

$$C_{T11} = 2C_T\left\{\frac{R_1 + R_2}{8a}\left(\alpha + \frac{\alpha - \sin\alpha}{(1 - \cos\alpha)}\right) + \frac{\alpha + \sin\alpha}{2(1 - \cos\alpha)}\left(\frac{R_1^2}{a^2}\ln\left(\frac{R_1}{R_2}\right) + \frac{R_2 - 3R_1}{2a}\right)\right\} \tag{34a}$$

$$C_{T12} = 2C_T\left\{\frac{R_1+R_2}{8a}\left(\alpha+\frac{\sin\alpha-\alpha}{(1-\cos\alpha)}\right)-\frac{\alpha+\sin\alpha}{2(1-\cos\alpha)}\left(\frac{R_1^2}{a^2}\ln\left(\frac{R_1}{R_2}\right)+\frac{R_2-3R_1}{2a}\right)\right\} \quad (34b)$$

$$C_{T13} = 2C_T\left\{-\frac{R_1+R_2}{8(R_1+R_2)}\left(\alpha+\frac{\alpha-\sin\alpha}{(1-\cos\alpha)}\right)+\frac{\alpha+\sin\alpha}{2(1-\cos\alpha)}\left(-\frac{R_1R_2}{a^2}\ln\left(\frac{R_1}{R_2}\right)+\frac{R_1+R_2}{2a}\right)\right\} \quad (34c)$$

$$C_{T14} = 2C_T\left\{-\frac{R_1+R_2}{8(R_1+R_2)}\left(\alpha+\frac{\sin\alpha-\alpha}{(1-\cos\alpha)}\right)+\frac{\alpha+\sin\alpha}{2(1-\cos\alpha)}\left(\frac{R_1R_2}{a^2}\ln\left(\frac{R_1}{R_2}\right)-\frac{R_1+R_2}{2a}\right)\right\} \quad (34d)$$

$$C_{T33} = 2C_T\left\{\frac{R_1+R_2}{8a}\left(\alpha+\frac{\alpha-\sin\alpha}{(1-\cos\alpha)}\right)+\frac{\alpha+\sin\alpha}{2(1-\cos\alpha)}\left(\frac{R_2^2}{a^2}\ln\left(\frac{R_1}{R_2}\right)+\frac{R_1-3R_2}{2a}\right)\right\} \quad (34e)$$

$$C_{T34} = 2C_T\left\{\frac{R_1+R_2}{8a}\left(\alpha+\frac{\sin\alpha-\alpha}{(1-\cos\alpha)}\right)-\frac{\alpha+\sin\alpha}{2(1-\cos\alpha)}\left(\frac{R_2^2}{a^2}\ln\left(\frac{R_1}{R_2}\right)+\frac{R_1-3R_2}{2a}\right)\right\} \quad (34f)$$

$$C_{T22}=C_{T11},\quad C_{T23}=C_{T14},\quad C_{T24}=C_{T13},\quad C_{T44}=C_{T33} \quad (34g)$$

By using the stress-displacement relationship, the shear forces at the nodes of soil element can be obtained as follows

$$\begin{bmatrix}T_r\\T_\theta\end{bmatrix} = 2C_T\begin{bmatrix}\frac{\partial}{\partial r}\\\frac{\partial}{r\partial\theta}\end{bmatrix}w_s \quad (35)$$

Table 2 Soil ring sector deformation matrix

		d_1	d_2	d_3	d_4
1	$\frac{\partial w}{\partial r}$	$-\frac{1}{a}$	0	$\frac{1}{a}$	0
	$\frac{\partial w}{r\partial\theta}$	$-\frac{b}{2R_2}$	$\frac{b}{2R_2}$	0	0
2	$\frac{\partial w}{\partial r}$	0	$-\frac{1}{a}$	0	$\frac{1}{a}$
	$\frac{\partial w}{r\partial\theta}$	$-\frac{b}{2R_2}$	$\frac{b}{2R_2}$	0	0
3	$\frac{\partial w}{\partial r}$	$-\frac{1}{a}$	0	$\frac{1}{a}$	0
	$\frac{\partial w}{r\partial\theta}$	0	0	$-\frac{b}{2R_1}$	$\frac{b}{2R_1}$
4	$\frac{\partial w}{\partial r}$	0	$-\frac{1}{a}$	0	$\frac{1}{a}$
	$\frac{\partial w}{r\partial\theta}$	0	0	$-\frac{b}{2R_1}$	$\frac{b}{2R_1}$

the matrix which relates the slopes at each nodes to nodal displacements is given in Table 2. where the following abbreviations are used.

$$a = R_1 - R_2 \tag{36}$$

$$b = \operatorname{cotan}\frac{\alpha}{2} \tag{37}$$

8. Computation of the mode shape parameter

The new mode shape parameter γ has to be obtained by Eq. (8), after determining the deformed shape $w(r, \theta)$ of the system. The integral terms of Eq. (8) can be evaluated for every plate and soil element separately. They are extended to the whole system by taking the summation of each element's contribution.

The deformed shape and its partial derivatives with respect to variable r and θ with an element can be given as

$$w = \sum_{i=1}^{n} w_i d_i \tag{38}$$

$$\frac{\partial w}{\partial r} + \frac{\partial w}{r\partial\theta} = \sum_{i=1}^{n}\left(\frac{\partial w_i}{\partial r} + \frac{\partial w_i}{r\partial\theta}\right)d_i \tag{39}$$

where the nodal freedoms of the element are known. Hence, the integral terms of an element

$$\iint w^2 dA = \iint\left(\sum_{i=1}^{n} w_i d_i\right)\left(\sum_{j=1}^{n} w_j d_j\right)dA = \sum_{i=1}^{n}\sum_{j=1}^{n}\left(\iint w_i w_j dA\right)d_i d_j \tag{40}$$

$$\iint\left[\left(\frac{\partial w}{\partial r}\right)^2 + \left(\frac{\partial w}{r\partial\theta}\right)^2\right]dA = \iint\left[\left(\sum_{i=1}^{n}\frac{\partial w_i}{\partial r}d_i\right)\left(\sum_{j=1}^{n}\frac{\partial w_j}{\partial r}d_j\right) + \left(\sum_{i=1}^{n}\frac{\partial w_i}{r\partial\theta}d_i\right)\left(\sum_{j=1}^{n}\frac{\partial w_j}{r\partial\theta}d_j\right)\right]dA \tag{41}$$

can be calculated using the $[C]$ and $[C_T]$ matrices which are already found.

$$\iint w^2 dA = \frac{1}{C}[d]^T[C][d] \tag{42}$$

$$\iint\left[\left(\frac{\partial w}{\partial r}\right)^2 + \left(\frac{\partial w}{r\partial\theta}\right)^2\right]dA = \frac{1}{2C_T}[d]^T[C_T][d] \tag{43}$$

The effects of all the elements can be summed up for the whole system, as follows:

$$\int_{r=0}^{\infty}\int_{\theta=0}^{2\pi} w^2 r dr d\theta = \sum_{el}\frac{1}{C}[d]^T[C][d] \tag{44}$$

$$\int_{r=0}^{\infty}\int_{\theta=0}^{2\pi}\left[\left(\frac{\partial w}{\partial r}\right)^2 + \left(\frac{\partial w}{r\partial\theta}\right)^2\right]r dr d\theta = \sum_{el}\frac{1}{2C_T}[d]^T[C_T][d] \tag{45}$$

As a result, the mode shape parameter can be obtained by using the above relations without requiring any additional algorithm.

8.1 Numerical example 1

Axially symmetric plates having various boundary conditions are analysed for various types of loading cases in order to check the convergence of the plate finite element developed by Saygun (1974), and results are given in Table 3 along with the results given by Szilard (1974) where $\rho = r/r_0$. In the numerical solution Poisson's ratio is taken 0.2 and the plate is divided six plate finite elements in radial direction. The angular width α of the element has not any effect in axially symmetric displacement case and can be taken any value.

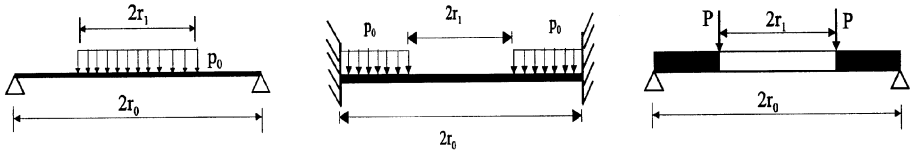

(a) (b) (b)

Fig. 3 Axial symmetric plates ($r_1/r_0 = 0.5$)

Table 3 Vertical displacements and bending moments

		$w\frac{p_0 r_0^4}{64D}$		$w\frac{Pr_0^2 r^1}{8D}$	$m_r\frac{p_0 r^2}{8}$	m_φ
	Plates	$\rho = 0.0$	$\rho = 0.5$	$\rho = 2/3$	$\rho = 1$	$\rho = 1$
a	Szilard (1974)	2.098	1.418			
	Saygun (1974)	2.098	1.418			
b	Szilard (1974)	0.361	0.238		–0.5625	–0.1125
	Saygun (1974)	0.361	0.239		–0.5539	–0.1108
c	Szilard (1974)			1.941		
	Saygun (1974)			1.942		

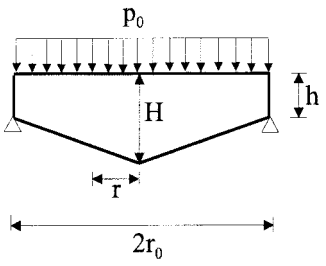

	Szilard (1974)	Saygun (1974)
$(w_{max})\frac{p_0 r_0^4}{EH^3}$	1.26	1.286

Fig. 4 Axial symmetric plate

8.2 Numerical example 2

Axially symmetric plate, of variable thickness subjected uniformly distributed load is analysed. Poisson's ration is 0.25 and plate is divided to four elements in radial direction and deflection at the center is given below (H/h = 1.5).

8.3 Numerical example 3

Circular plate, which is shown in Fig. 5 under the concentrated load at the centre and supported at three points, is analysed by using the symmetry conditions, i.e., only one third of the plate is considered. In solution Poisson's ratio is taken 0.25 and plate is divided to six element in radial direction and four element in angular direction. Central displacement is given below.

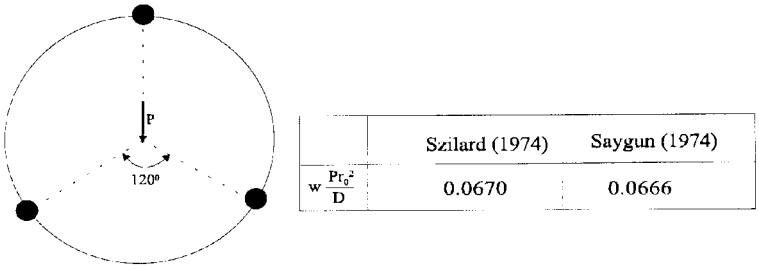

Fig. 5 Circular plate suported at three points

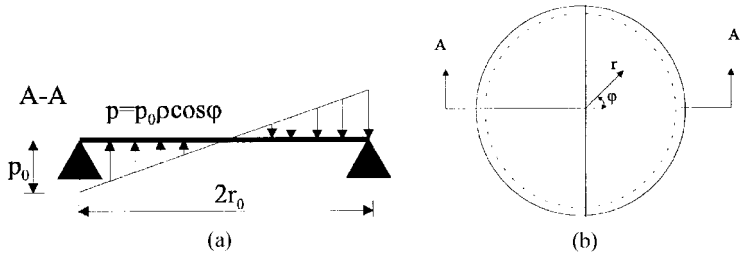

Fig. 6 Structural system and loading

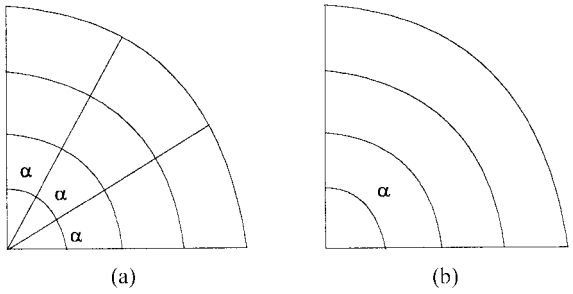

Fig. 7 Fiuite element mesh

Table 4 Vertical displacements and bending moments

		Szilard (1974)	Saygun (1974)	
			$\alpha = 30$	$\alpha = 90$
$\rho = 1/4$ $\varphi = 0^o$	w (cm)	0.14583	0.14564	0.14569
	M_r	0.40625	0.41921	0.41934
	M_θ	0.20625	0.20766	0.20764
$\rho = 1/2$ $\varphi = 0^o$	w (cm)	0.21333	0.21319	0.21323
	M_r	0.65000	0.67583	0.67620
	M_θ	0.35000	0.35475	0.35431
$\rho = 3/4$ $\varphi = 0^o$	w (cm)	0.15750	0.15744	0.15746
	M_r	0.56875	0.60784	0.60764
	M_θ	0.36880	0.37639	0.37591

8.4 Numerical example 4

In this example circular plate, shown in Fig. 6 subjected by load $p = p_0\rho\cos\varphi$, is analysed. Using symmetry and antisymmetry properties only one fourth of the plate is considered. Plate is divided to four elements in radial direction and three element ($\alpha = 30$, Fig. 7a) then one element ($\alpha = 90$, Fig. 7b) in angular direction. In this example load matrices of elements are obtained numerically by using the integral formula $P_i = \int\int p w_i r d\theta dr$. Resultant vertical displacements and bending moments are given in Table 4 where the following dimensions are used $v = 0.20$, and $D = 468.75$ tm.

The results obtained in this study and given by Szilard (1974) are quite in agreement. Since the displacement function expressed at (16) satisfies the first harmonique deflection case, the number of elements along the angular direction does not change the results and even one element is sufficient.

8.5 Numerical example 5

Circular tank foundation investigated by Vallabhan and Das (1991) for various loading cases is analysed to check the convergence of plate and soil element on the two-parameter foundation. Ring sector finite elements are used for the plate as well as the for the soil. The mode shape parameter γ calculated and given comparatively with the results of Vallabhan. As can be seen, the two results are in good agreement. The numerical values of the parameter are assumed to be.

· Radius of the plate R = 10 ft (3.05 m).
· Modulus of elasticity of the plate $E_p = 3 \times 10^6$ psi (22.7 GPa)
· Poisson's ratio of the plate $v_p = 0.2$.
· Thickness of the plate h = 0.8 ft (0.24 m).
· Depth of the soil foundation H= 10 ft (3.05 m).
. Modulus of elasticity of the soil =3 x 10^3 psi (22.7 MPa)
. Poisson's ratio of the soil $v_s = 0.2$

Loading case 1. A uniformly distributed load = 500 psf (26.3 kN/m^2)

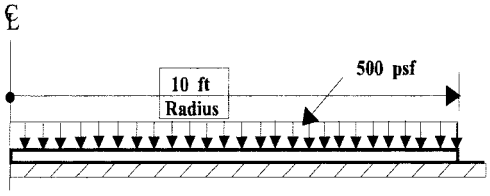

	γ
Vallabhan	0.915
Present study	0.915

Fig. 8 Uniformly load case

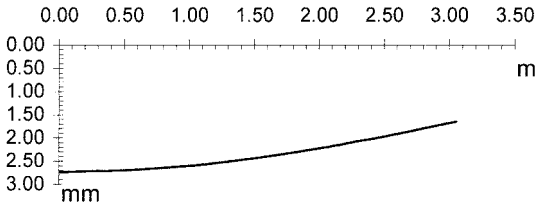

Fig. 9 Vertical displacements of circular plate due to uniformly distributed load

Loading case 2. An edge load Q = 1000 p/ft (16 kN/m).

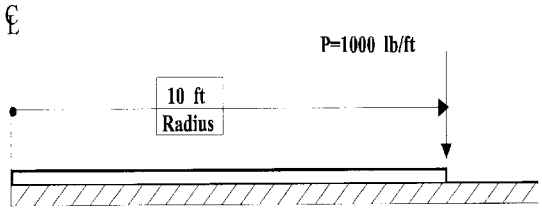

	γ
Vallabhan	1.49
Present study	1.52

Fig. 10 Edge load

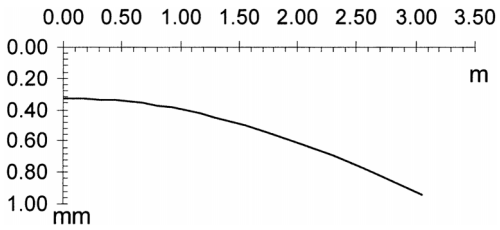

Fig. 11 Vertical displacements of circular plates due to concentrated edge load

Loading case 3. An edge moment M = 10,000 p-ft/ft (523.5 kN-m/m)

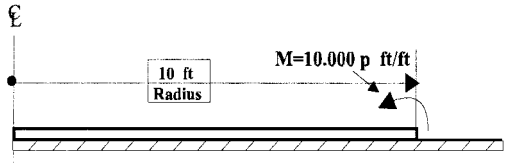

	γ
Vallabhan	2.94
Present study	3.04

Fig. 12 Edge moment

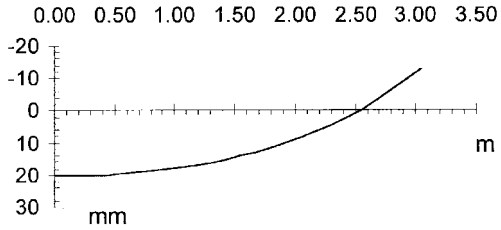

Fig. 13 Vertical displacements of circular plate due to edge moment

8.6 Numerical example 6

Circular plate on two-parameter elastic foundation shown in Fig. 14 is analysed, where the following parameters are used:

· Modulus of elasticity of the plate $E_p = 2.10^7$ kN/m^2
· Poisson's ratio of the plate $\nu_p = 0.16$

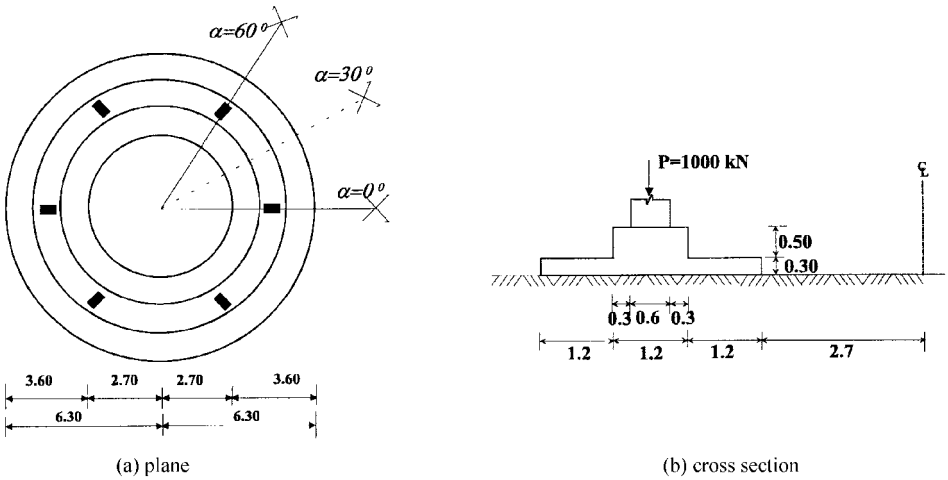

Fig. 14 Structural system and cross section

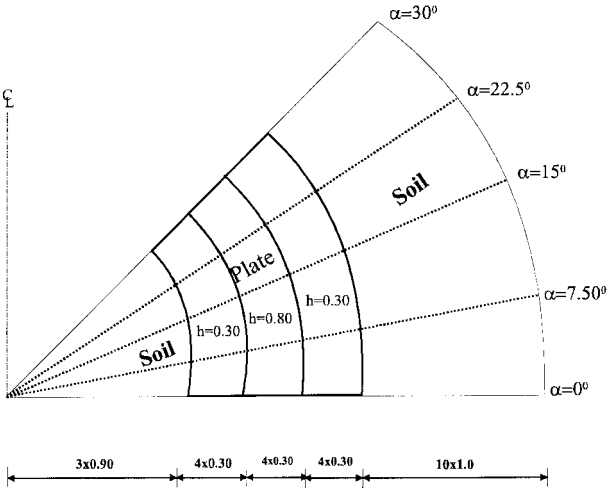

Fig. 15 Finite element mesh

Table 5 Mode shape parameter and soil coefficients

ν	γ	$C\left(\frac{kN}{m^3}\right)$	$C_T\left(\frac{kN}{m}\right)$
0.25	1.323	10081.85	43404.87

· Modulus of elasticity of the soil E_s = 80.000 kN/m^2
· Poisson's ratio of the soil ν_s = 0.25
· Depth of the soil foundation H = 10 m

The finite element mesh used in the analysis is given in Fig. 15 where the extension region of the soil is taken equal to the thickness of the compressible layer. Concentrated loads are taken as 0.60 m length line loads in radial direction. The interior radius is taken small value (R_2 = 0.001 m) in order to apply the finite element developed without requiring a three-node element. This way one can avoid that some of the coefficients of the matrices [C] and [C_T] become undetermined when the interior radius is equal to zero.

The boundary conditions due to axial symmetry at line $\alpha = 0^o$ and $\alpha = 30^o$ are will be as follows

$$w_i \neq 0, \quad \frac{\partial w}{\partial r} \neq 0, \quad \frac{\partial w}{r\partial\theta} = 0, \quad \frac{\partial}{\partial r}\left(\frac{\partial w}{r\partial\theta}\right) = 0$$

The value of mode shape parameter (γ) and soil coefficients are shown in Table 5.

The variation of vertical displacements and bending moments M_r and M_θ are shown along the axis $\alpha = 0$ and $\alpha = 30$ in Figs. 16-21.

The plate on the Winkler soil and on the two-parameter soil are analysed separately and vertical displacements are plotted. The comparison of the vertical displacement demonstrates that by taking into account the shear parameter in addition to the Winkler assumption, the vertical displacements decrease and the shear forces on the boundaries take on larger values. The variation of bending

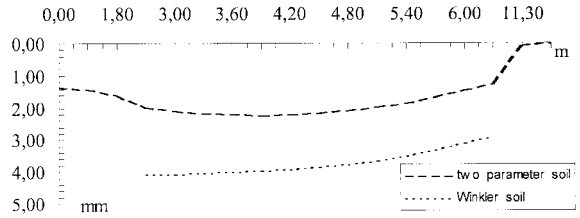

Fig. 16 Variation of the deflection of the plate for $\alpha = 0$

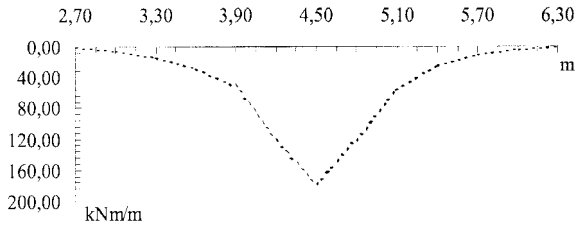

Fig. 17 Variation of bending moment M_r for $\alpha = 0$ in the case of the two-parameter foundation

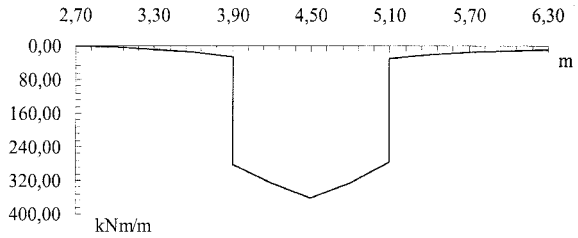

Fig. 18 Variation of bending moment M_θ for $\alpha = 0$ in the case of two parameter foundation

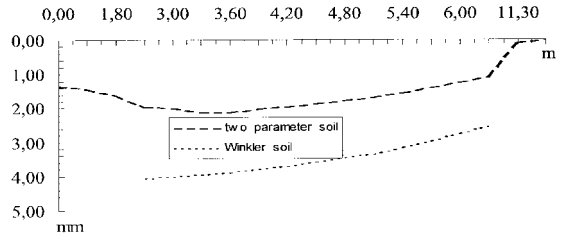

Fig. 19 Variation of the deflection of the plate for $\alpha = 30$

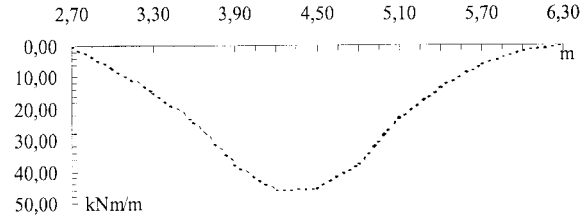

Fig. 20 Variation of the bending moment M_r for $\alpha = 30$ in the case of the two-parameter foundation

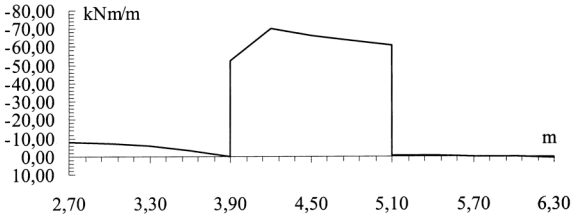

Fig. 21 Variation of the bending moment M_θ for $\alpha = 30$ in the case of the two parameter foundation

moment M_θ in circular ring differs from rectilinear beams on two parameter foundation. It can be seen that, negative bending moment decreases in the middle of the plate and positive moment increases at the span support. The rotation $\partial w / \partial r$ of the ring causes an additional positive constant M_θ moment.

9. Conclusions

In the present study circular plates on a two-parameter elastic foundation are analysed by inclusion of soil parameter effects to the sector plate finite element developed by Saygun (1974). Sector soil finite elements are used in addition to plate finite element. The displacements for the plate-soil system , the bending and twisting moments for the plate and soil stresses can be computed and compared with the existing results. The elastic bedding and shear parameter coefficients of the

soil are obtained by using the elastic constant, the thickness of the compressible layer and the mode shape parameter. Due to the interaction between the plate and the soil, the mode shape parameter also depends on the shape and the dimension of the plate and the elastic constant of the soil.

References

Brown, P.T. (1969), "Numerical analysis of uniformly loaded circular rafts on an elastic layer of finite depth", *Geotechnique*, **19**, 301-306.

Çelik, M. and Saygun, A.I. (1999), **"**A method for the analysis of plates on two parameter foundation", *Int. J. Solids Struct.*, **36**, 2891-2916.

Çelik, M. (1996), **"**Plate finite element formulation including shear deformation and a method for the analysis of plate on two parameter foundation", Ph.D. Thesis, Istanbul Technical University, (in Turkish.)

Jones, R. and Xenophontos, J. (1977), "The Vlasov foundation model", *Int. J. Mech. Sci.*, **19**, 317-323.

Pasternak, P.L. (1954), *On a New Method of Analysis of an Elastic Foundation by Means of Two Foundation Constants*, Gosudarstvennoe Izdatelstvo Literaturi po Stroitelstvu i Arkhitekture, Moscow (in Russian).

Saygun, A.I. (1974), "Curved elements for the analysis of plates and shells", Ph. D. Thesis, Istanbul Technical University, (in Turkish).

Szilard, R. (1974), *Theory and Analysis of Plates, Classical and Numerical Methods*. Prentice-Hall, Englewood, New Jersey.

Vallabhan, C.V.G. and Das, Y.C. (1991), "Refined model for analysis of plates on elastic foundations", *J. Eng. Mech.*, **117**, 2830-2844.

Vallabhan, C.V.G. and Das. Y.C. (1988), "Parametric study of beams on elastic foundations", *J. Eng. Mech.*, **114**, 2072-2082 .

Vallabhan, C.V. and Das, Y.C. (1991). "A refined model for beams on elastic foundations", *Int. J. Solid Struct.*, **27**, 629-637.

Vallabhan, C.V.G., Straughan, W.T. and Das, Y.C. (1991), "Refined model for analysis of plates on elastic foundations", *J. Eng. Mech.*, **117**, 2830-2844.

Vallabhan, C.V. and Daloğlu, A.T. (1997), "Consistent FEM-Vlasov model for slabs on elastic foundations", *Seventh International Conference on Computing in Civil and Building Engineering*, 19-21 August, Seoul, Korea, pp.57-62.

Vallabhan, C.V. and Das, Y.C. (1991), "Analysis of circular tank foundation", *J. Eng. Mech.*, **117**, 789-797.

Vlasov, V.Z. and Leont'ev, U.N. (1966), "Beams, plates, and shells on elastic foundation", Israel Program for Scientific Translation, Jerusalem.